



## PAPER

## RoWDI: rolling window detection of sleep intrusions in the awake brain using fMRI

RECEIVED  
19 May 2021REVISED  
29 September 2021ACCEPTED FOR PUBLICATION  
30 September 2021PUBLISHED  
19 October 2021Govinda R Poudel<sup>1,2,\*</sup> , Stephanie Hawes<sup>1</sup>, Carrie R H Innes<sup>2,3</sup>, Nicholas Parsons<sup>5</sup>, Sean P A Drummond<sup>4</sup>, Karen Caeyensberghs<sup>5</sup> and Richard D Jones<sup>2,3,6,7</sup><sup>1</sup> Mary Mackillop Institute for Health Research, Faculty of Health Sciences, Australian Catholic University, Melbourne, Australia<sup>2</sup> New Zealand Brain Research Institute, Christchurch, New Zealand<sup>3</sup> Department of Medicine, University of Otago, Christchurch, New Zealand<sup>4</sup> Turner Institute for Brain and Mental Health, Monash University, Melbourne, Australia<sup>5</sup> Cognitive Neuroscience Unit, School of Psychology, Deakin University, Melbourne, Australia<sup>6</sup> Department of Electrical and Computer Engineering, University of Canterbury, Christchurch, New Zealand<sup>7</sup> School of Psychology, Speech and Hearing, University of Canterbury, Christchurch, New Zealand

\* Author to whom any correspondence should be addressed.

E-mail: [Govinda.poudel@acu.edu.au](mailto:Govinda.poudel@acu.edu.au)**Keywords:** sleep, drowsiness, local sleep, vigilance, mental fatigue, sleep deprivationSupplementary material for this article is available [online](#)**Abstract**

*Objective.* Brief episodes of sleep can intrude into the awake human brain due to lack of sleep or fatigue—compromising the safety of critical daily tasks (i.e. driving). These intrusions can also introduce artefactual activity within functional magnetic resonance imaging (fMRI) experiments, prompting the need for an objective and effective method of removing them. *Approach.* We have developed a method to track sleep-like events in awake humans via rolling window detection of intrusions (RoWDI) of fMRI signal template. These events can then be used in voxel-wise event-related analysis of fMRI data. To test this approach, we generated a template of fMRI activity associated with transition to sleep via simultaneous fMRI and electroencephalogram (EEG) ( $N = 10$ ). RoWDI was then used to identify sleep-like events in 20 individuals performing a cognitive task during fMRI after a night of partial sleep deprivation. This approach was further validated in an independent fMRI dataset ( $N = 56$ ). *Main results.* Our method (RoWDI) was able to infer frequent sleep-like events during the cognitive task performed after sleep deprivation. The sleep-like events were associated with on average of 20% reduction in pupil size and prolonged response time. The blood-oxygen-level-dependent activity during the sleep-like events covered thalamic-cortical regions, which although spatially distinct, co-existed with, task-related activity. These key findings were validated in the independent dataset. *Significance.* RoWDI can reliably detect spontaneous sleep-like events in the human brain. Thus, it may also be used as a tool to delineate and account for neural activity associated with wake-sleep transitions in both resting-state and task-related fMRI studies.

**1. Introduction**

Brief episodes of sleep can intrude into wakefulness when the homeostatic sleep drive is elevated due to sleep loss, mental fatigue, or drowsiness [1–5]. Recent evidence suggests that sleep-like intrusions are also common in cognitive neuroimaging experiments using functional magnetic resonance imaging (fMRI) and forms a major source of artefactual activity and

connectivity during both task-based and resting-state fMRI paradigms [6]. fMRI is particularly useful for characterising the dynamic properties of the human brain network [7]. However, intrusions of sleep can represent an important confound for which there is currently no identification or removal technique available [8]. A recent resurgence of the debate surrounding fMRI reliability has highlighted the importance of removing spurious signal intrusions that may

be driving subsequent activity and functional connectivity findings [9].

Peripheral recordings such as EEG monitoring can be used to detect intrusions of sleep episodes [10]. Pupillometric recordings have also been used extensively in neuroimaging studies as a marker of changes in arousal [11–14]. Increased theta waves (4–7 Hz theta) that replace higher-frequency alpha waves (>8 Hz) on EEG recordings are considered to be due to microsleeps (brief stage-1 sleep) associated with extreme sleepiness [15, 16]. In individuals performing cognitive tasks, sleep intrusions can also lead to response lapses and performance errors [16]. Slow eye-lid closures can also indicate transition to sleep whilst awake [1, 17, 18]. However, most of these peripheral recordings are cumbersome to collect during fMRI scanning and require post-hoc subjective rating of the data. Thus, methods to automatically track intrusions of sleep-like activity are highly desirable.

fMRI studies have shown that the sleep-like state can transiently alter blood-oxygen-level-dependent (BOLD) fMRI signal [6, 19–21]. Striking patterns of BOLD signal co-activation deactivation have been associated with spontaneous slow-eye-closures, and microsleeps, which can frequently occur when drowsy [1, 17, 18, 22]. The fMRI amplitude fluctuations in specific brain networks can therefore be used to track moment-to-moment variations of alertness states in mammals [19, 20, 23]. Such large-scale co-activation patterns can also intrude into resting-state BOLD fMRI data, reflecting momentary reductions in arousal during the awake resting state and task performance [20, 23].

Here, we introduce an fMRI-based framework to infer intrusions of sleep-like activity in the awake humans performing a cognitive task. Simultaneous fMRI and EEG were used to derive a spatial map of activity associated with transition to early sleep. A rolling window detection of intrusions technique (RoWDI) was then implemented to infer the intrusions of the sleep-like fMRI activity map in awake, but sleep-deprived, humans performing a cognitive task. The key findings were also validated using an independent fMRI dataset.

## 2. Methods

### 2.1. Data acquisition

In this study we used data from three studies to develop, test, and validate our method. The first study acquired simultaneous fMRI and EEG data, which was necessary to generate spatial maps of fMRI activity associated with increased EEG theta activity (4–7 Hz). The second study acquired fMRI data from partially sleep-deprived participants, who were more likely to experience sleep-like episodes—a condition necessary for detecting sleep-like events using

our method. The third study was for validation and used an openly available fMRI data acquired from sleep-deprived individuals. The data acquisition for these studies is described below.

#### 2.1.1. Simultaneous fMRI + EEG study

Simultaneous fMRI and EEG recordings were obtained from 12 healthy participants (6 female; age: 19–27; right-handed) during a 40 min daytime nap session inside a 3T MRI scanner (Siemens Skyra). The 40 min scan was divided into four runs of 10 min each with ~10–15 s of pause between the scans. Of these, ten participants completed the full simultaneous fMRI and EEG session. To facilitate stage 1 sleep within the MRI environment, the experiment was performed following a substantial lunch and the participants were instructed to keep their eyes closed and sleep.

fMRI data were acquired using a gradient-echo echo planar imaging (EPI) acquisition that covered most of the brain (slice thickness =  $3.3 \times 3.3 \times 3.3$  mm, repetition time (TR) = 2.5 s, TE = 40 ms, Flip angle (FA) =  $90^\circ$ , total scan time = 40 min, number of slices = 38).  $T_1$ -weighted anatomical images were acquired using sagittal scanning 3D MPRAGE sequence (Echo time (TE) = 2.07 ms; TR = 2.3 s; field of view:  $256 \times 256$  mm; slice thickness: 1 mm; FA = 9; TI = 900, 176 slices). Simultaneous EEG data were acquired using a 64-channel MR-compatible EEG system (BrainProducts, Germany) as per best practice [24].

#### 2.1.2. fMRI and pupillometric study

In a second study, fMRI and eye-video data were acquired from 20 healthy right-handed adults (10 females) aged between 20 and 37 years ( $M = 24.9$ ,  $SD = 4.2$ ). The participants were partially sleep-deprived (4 h time in bed) and performed a two-choice logical decision-making task during fMRI scanning. In this task, the participants were presented with a set of cards on a screen such that if the two cards are the same for any feature (colour, number, symbol, or shading) and one is not, then the three cards are not a set, otherwise they are a set. The participants responded ('yes') or right ('no') on whether cards were a set using an MRI-compatible button box. Experimental stimuli were presented on a screen for 5.0 s, followed by a fixation cross for 2.5–10 s ( $M = 4.0$ , jittered). Each participant completed three runs of 6 min duration. Each run consisted of 40 experimental stimuli and 40 fixation crosses (total trials = 120 in 3 runs). Response time (RT) was recorded for each trial.

MRI data were acquired using a 3T scanner. fMRI data were obtained using EPI sequence (TR = 2.5 s; number of repetitions = 293; TE = 35 ms; field of view =  $220 \times 220$  mm; number of slices = 37; slice

thickness = 4.5 mm; matrix =  $64 \times 64$ ). Structural MRI scans (1 mm isotropic) were also acquired.

Eye-video data were captured whilst participants completed the task inside the MRI. Right-eye movement was recorded on a Visible Eye™ system (Avotec Inc., Stuart, FL) mounted on the head-coil of the MRI scanner. Custom-built video recording software and a video-capture card was used to record eye-videos onto a computer at 25 frames  $s^{-1}$  ( $350 \times 280$  px).

### 2.1.3. Validation data

An independent dataset from the Stockholm Sleep Brain Study was used for validation purpose. The fMRI data from  $N = 56$  partially sleep-deprived participants who participated in a 8 min scanning session in which the participants were asked to rate their sleepiness every 2 min with the Karolinska Sleepiness Scale was used. The dataset is available via OpenNeuro database (ds000201). The experimental protocol for the study is published elsewhere [25].

## 2.2. Data processing

### 2.2.1. Processing of EEG data

The EEG data from the first study were first processed and analysed using Brain Vision Analyser and Matlab R2018a, (Mathworks, MA, USA) to remove the gradient and ballistocardiogram artefacts (see supplementary materials (available online at [stacks.iop.org/JNE/18/056063/mmedia](https://stacks.iop.org/JNE/18/056063/mmedia))). Denoised EEG data were analysed using a moving window of 2.5 s, yielding a spectrogram for each electrode via Welch's periodogram method. We generated a time-frequency vector of power in theta (4–7 Hz, i.e. similar to non rapid eye movement (NREM) sleep stage 1) and alpha (8–13 Hz, relaxed wakefulness) from the EEG data. Average power spectral densities (PSDs) in the theta (4–7 Hz) and alpha (8–13 Hz) bands were estimated for nine occipito-parietal EEG electrodes (O1, O2, OZ, P1, P2, PZ, PO3, PO4, POZ), at each MRI TR (figure 1(A)). The PSD distribution at these electrodes was within the theta-alpha band (4–13 Hz) (figures 1(B) and (C)). These electrodes were chosen because of the evidence showing relative increase in posterior theta power during sleep onset [26].

### 2.2.2. Processing of fMRI data

The fMRI data from all three studies were pre-processed using FSL (FMRIB's Software Library, [www.fmrib.ox.ac.uk/fsl](http://www.fmrib.ox.ac.uk/fsl)), Advanced Normalisation Tools (ANTs) (<http://stnava.github.io/ANTs/>), and custom Linux Shell and Matlab scripts (Matlab 7.6.0, R2018a, Mathworks, MA, USA). Data pre-processing steps (supplementary material) included (a) motion correction, (b) slice-time correction, (c) spatial smoothing (6 mm Gaussian kernel), and (d) high-pass filtering with a cut-off of 256 s. The fMRI data were normalized to the  $2 \times 2 \times 2$  mm<sup>3</sup>

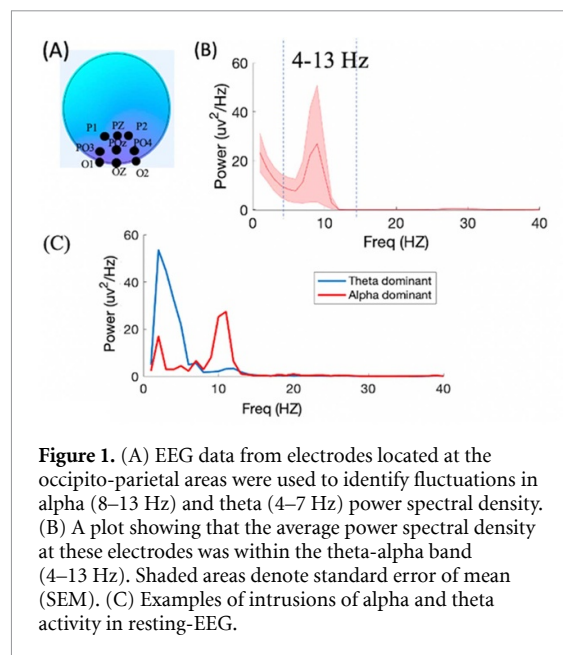


**Figure 1.** (A) EEG data from electrodes located at the occipito-parietal areas were used to identify fluctuations in alpha (8–13 Hz) and theta (4–7 Hz) power spectral density. (B) A plot showing that the average power spectral density at these electrodes was within the theta-alpha band (4–13 Hz). Shaded areas denote standard error of mean (SEM). (C) Examples of intrusions of alpha and theta activity in resting-EEG.

Montreal Neurological Institute template using linear and non-linear registration available in ANTs (see supplementary materials).

### 2.2.3. Generation of fMRI activity map associated with EEG theta

In the first study, the EEG alpha and theta time series were used as regressors in a general linear model analysis of the fMRI data (supplementary materials). For each individual subject, EEG alpha, EEG theta, large motion outliers, and six motion parameter regressors were used in a linear regression model, which was fitted to the data in a voxel-wise manner. The regression model was estimated at the first level for each participant, generating parameter estimates maps of activity for each subject. A group-level one-sample  $t$ -test was performed using non-parametric statistics (FSL randomize) with 5000 permutations. The main-effects of alpha and theta on fMRI activity were considered significant at  $p < 0.05$  (family-wise-error corrected using cluster thresholding at  $z > 2.3$ ). The spatial map of fMRI activity associated with EEG theta were used as template in the implementation of RoWDI.

### 2.2.4. Processing of the eye-video data

The eye-videos were processed using the starburst algorithm to detect pupil from the dark-pupil infrared illuminated eye videos [27]. The algorithm determines the best-fitting ellipse using consensus set and optimizes the ellipse parameters using model based techniques [27]. The starburst algorithm was able to detect pupil when eyes open fully and partially open. The pupil size was set to 0 when it could not be detected due to eye-closure. Relative change in pupil size is a good indicator of changes in arousal

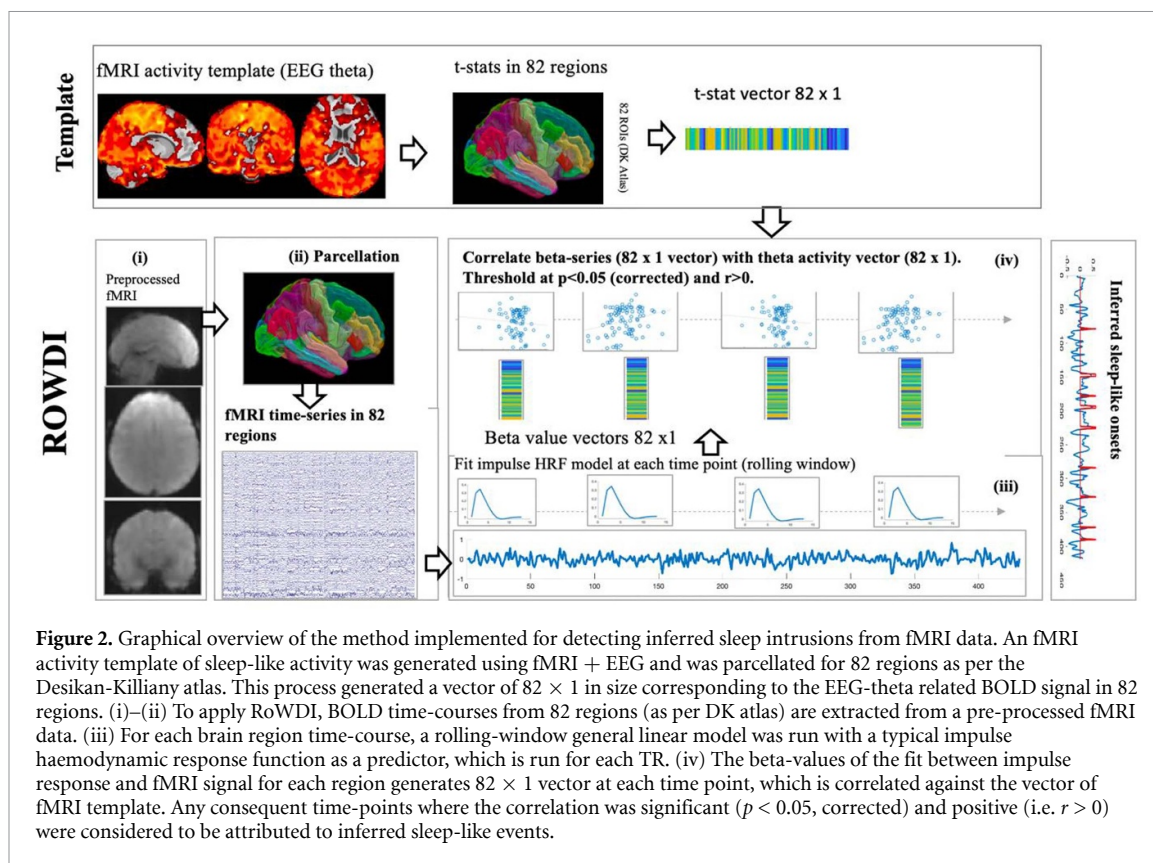


**Figure 2.** Graphical overview of the method implemented for detecting inferred sleep intrusions from fMRI data. An fMRI activity template of sleep-like activity was generated using fMRI + EEG and was parcellated for 82 regions as per the Desikan-Killiany atlas. This process generated a vector of  $82 \times 1$  in size corresponding to the EEG-theta related BOLD signal in 82 regions. (i)–(ii) To apply RoWDI, BOLD time-courses from 82 regions (as per DK atlas) are extracted from a pre-processed fMRI data. (iii) For each brain region time-course, a rolling-window general linear model was run with a typical impulse haemodynamic response function as a predictor, which is run for each TR. (iv) The beta-values of the fit between impulse response and fMRI signal for each region generates  $82 \times 1$  vector at each time point, which is correlated against the vector of fMRI template. Any consequent time-points where the correlation was significant ( $p < 0.05$ , corrected) and positive (i.e.  $r > 0$ ) were considered to be attributed to inferred sleep-like events.

[11–14] hence we estimated the time-course of pupil size at the onset of inferred sleepiness by calculating baseline corrected time-locked pupil size. An example of pupil size data for a participant is provided in the supplementary figure 1. Percentage of 0 values in each subject is available in the supplementary table 3.

### 2.3. RoWDI

Previous studies have demonstrated that lowered arousal and early sleep is associated with an archetypical spatial pattern of fMRI activity [28–30]. Hence, we postulated that by monitoring intrusions of the fMRI maps associated with increased EEG-theta, we may be able to infer sleep-like intrusions in the fMRI data without the need for simultaneous EEG recordings. Thus, we implemented a method to track EEG-theta fMRI activity patterns in any fMRI dataset. A graphical overview of the implementation of RoWDI is provided in figure 2.

First, we used the template of fMRI activity associated with EEG theta obtained from the first study and generated an average theta-related fMRI activity vector in 82 brain regions mapped using the cortical and sub-cortical parcellations from the Desikan-Killiany atlas. A rolling window general linear regression model was then employed to identify any transient fMRI activity in a pre-processed fMRI data.

The transient event-related fMRI activity was modelled as a typical haemodynamic response function with span of 32.5 s. At each time-point, this model was fit to the data using a general linear model. By using a rolling-window regression, we identified parameter estimates of the fit between the transient fMRI model and the denoised fMRI data in each of the 82 regions, resulting in  $82 \times 1$  vectors of parameter estimates at each time point. These parameter estimates were then correlated (Pearson's correlation) with the  $82 \times 1$  vector of fMRI activity associated with EEG-theta activity, which provided an estimate of how well the transient activity at each time-point represents sleep-like activity. Any time-points where the correlation was significantly high ( $p < 0.05$ , corrected) and positive (i.e.  $r > 0$ ) were inferred to be due to sleep-like intrusions. Consequent significant time-points of longer than one TR were considered to be a single event.

### 2.4. Voxelwise analysis of fMRI data

The sleep-like events identified using RoWDI were used in multi-level voxel-wise generalized linear model analysis of fMRI data (from the second and validation data) to identify spatial distribution of brain activity due to task and sleep-like onsets. To analyse the data from the second study, a first-level general linear model was implemented. This model included

predictors for (a) a task-related regressor (120 trials across 3 runs) of modelled epochs of task-related activity, with the height of the response modulated by RT, (b) inferred sleep intrusions modelled as impulse activity convolved with a double-gamma haemodynamic response function, (c) response errors modelling the time points when subjects failed to respond during the task, (d) six motion parameters, and (e) large motion outliers. For each subject, the main effects of task and sleep like intrusions were estimated using first-level contrasts representing average activity. For second-level group analysis, a non-parametric approach was used to estimate group-level significance of the first-level parameter estimates. A group-level  $t$ -test was performed using non-parametric statistics (FSL Randomize) and 5000 permutations. The main-effect of tasks was considered significant at  $p < 0.05$  (voxel-level family-wise-error corrected). The main-effect of inferred sleep intrusions was considered significant at  $p < 0.05$  (cluster corrected,  $z$ -threshold  $> 4$ ).

For the validation data, the fMRI data was analysed in a similar manner as described above. A detailed description is provided in supplementary material.

### 3. Results

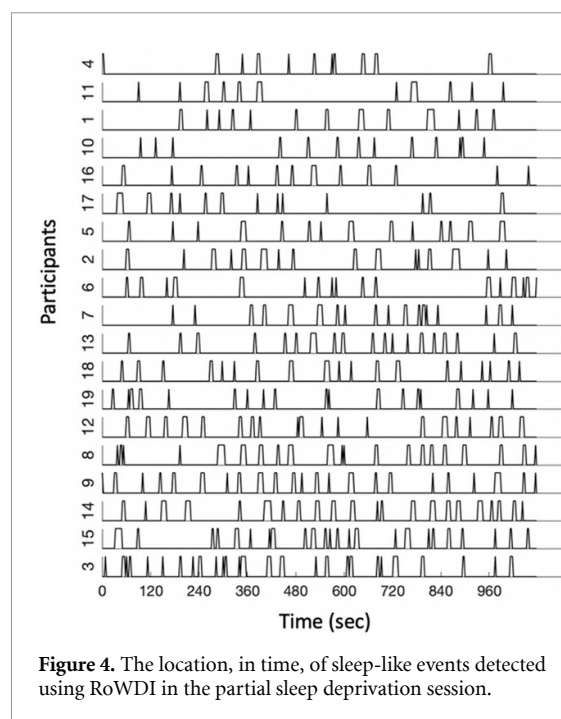
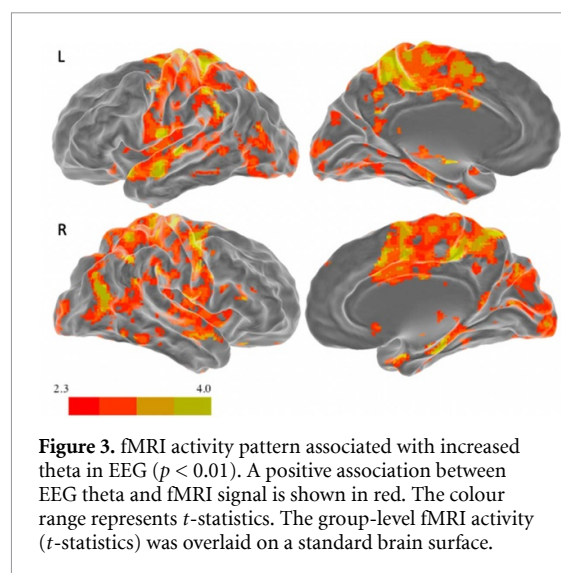
#### 3.1. A map of fMRI activity associated with transition to sleep

The fMRI map/template of positive association ( $p < 0.01$ ) between power in theta band of EEG and fMRI signal is shown in figure 3. After cluster-based correction ( $Z > 2.3$ ), significant association was observed in the bilateral precuneus, superior parietal lobule, precentral gyrus, postcentral gyrus, and superior frontal gyrus (supplementary table S1).

#### 3.2. Frequent sleep-like intrusions in awake brain

When the fMRI template of EEG-theta was used, RoWDI detected frequent intrusions of these activity maps in the individuals performing the decision making task after sleep deprivation (10–27;  $M = 17$ ,  $SD = 4.7$ ). The location of these events in time is provided in figure 4.

The average pupillometric profile of these sleep-like events inferred from fMRI data is shown in figure 5(A). There was, on average, a 20% reduction in pupil size during the sleep-like events, suggesting that these events were indeed associated with reduction in arousal. Furthermore, the decision trials which coincided with inferred sleep intrusions had longer average RT compared to the other trials ( $t(18) = 2.21$ ,  $p = 0.04$ ). There was also a positive correlation between total duration of sleep-like intrusions and average reaction time ( $r = 0.53$ ,  $p = 0.02$ ) (figure 5(B)).



#### 3.3. fMRI activity associated with sleep-like events and task trials

General linear model analysis of the sleep-like events and decision-making trials revealed significant and distinct fMRI activity ( $p < 0.05$ , corrected). Task-related activity was observed in the bilateral prefrontal (inferior/middle), motor (precentral/postcentral), parietal (superior), anterior and posterior cingulate and bilateral insula cortically, and the bilateral thalamus and striatum subcortically. Whereas, inferred sleep intrusions were associated with increased activity in the bilateral visual areas (occipital pole, cuneus, lingual gyri), auditory areas (superior temporal gyri, Heschl's gyri), primary and secondary somatosensory areas (postcentral gyri, parietal operculum, superior parietal lobule, and

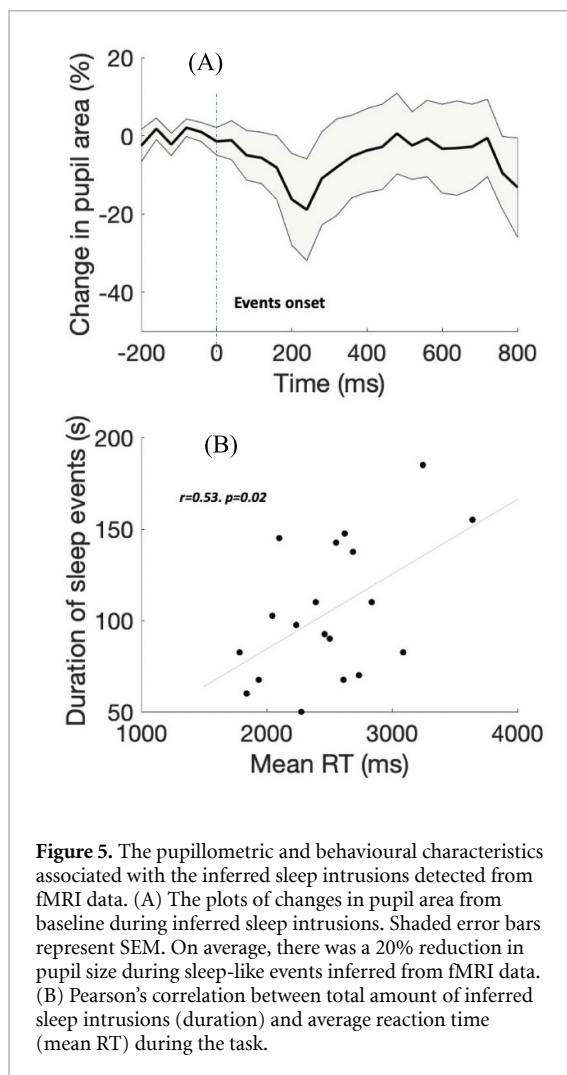


**Figure 5.** The pupillometric and behavioural characteristics associated with the inferred sleep intrusions detected from fMRI data. (A) The plots of changes in pupil area from baseline during inferred sleep intrusions. Shaded error bars represent SEM. On average, there was a 20% reduction in pupil size during sleep-like events inferred from fMRI data. (B) Pearson's correlation between total amount of inferred sleep intrusions (duration) and average reaction time (mean RT) during the task.

insular cortex), the primary motor areas (precentral gyri), supplementary motor areas, default-mode areas (including the bilateral precuneus, angular gyri), and limbic areas (encompassing the bilateral parahippocampi) (figure 6 and supplementary table 2).

Decreased activity during sleep-like events was observed in subcortical areas including the bilateral thalamus, caudate, and putamen, and cortical areas such as the rostral anterior cingulate gyrus (basal forebrain), rostral middle-frontal gyrus, and lateral inferior parietal areas.

### 3.4. Validation of RoWDI

The RoWDI approach identified frequent intrusions of sleep-like events in the partially sleep-deprived participants from an independent fMRI dataset. Importantly, when these events were used in the voxel-wise fMRI analysis, a pattern of co-activation and de-activation was observed, which replicated the pattern observed during sleep-like intrusion in the decision-making task (supplementary figure 2). Data processing and analysis for the validation is provided in supplementary materials.

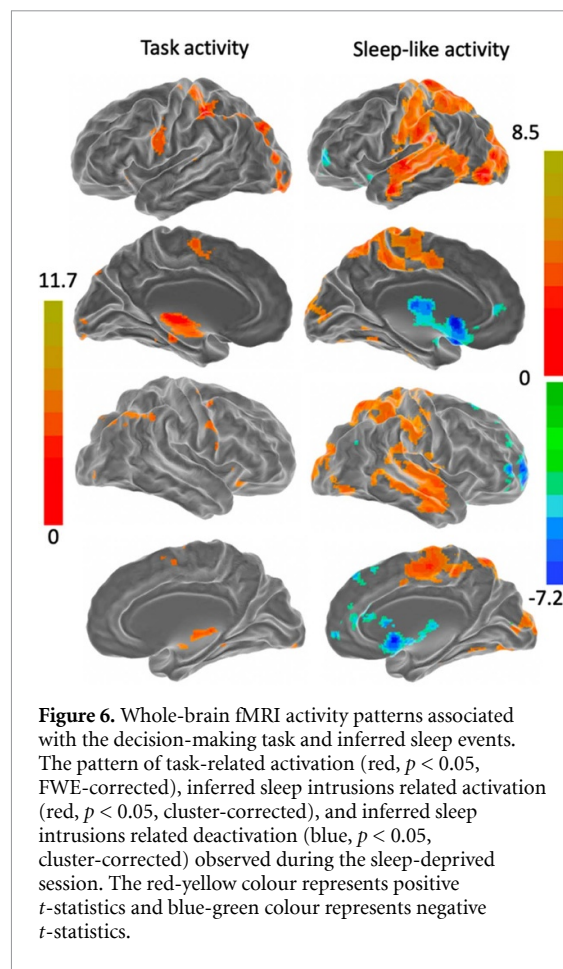


**Figure 6.** Whole-brain fMRI activity patterns associated with the decision-making task and inferred sleep events. The pattern of task-related activation (red,  $p < 0.05$ , FWE-corrected), inferred sleep intrusions related activation (red,  $p < 0.05$ , cluster-corrected), and inferred sleep intrusions related deactivation (blue,  $p < 0.05$ , cluster-corrected) observed during the sleep-deprived session. The red-yellow colour represents positive  $t$ -statistics and blue-green colour represents negative  $t$ -statistics.

## 4. Discussion

We have developed a novel method to detect intrusions of sleep-like events using fMRI data in awake humans. Our results can be summarized into three main findings: (a) RoWDI can reliably detect sleep-like intrusions in awake humans using fMRI data alone, (b) these sleep-like intrusions are associated with pupillometric markers of reduced arousal and slowed RTs, and (c) they are associated with a transient pattern of activation and de-activation in brain networks distinct from co-existing task-related brain regions.

Simultaneous fMRI + EEG recordings were used to derive a spatial map of BOLD fMRI activity associated with an increase in EEG activity in the theta band—a hallmark of EEG associated with transition to sleep. Importantly, the fMRI activity map associated with EEG theta covered occipito-parietal cortices, consistent with previous studies showing similar changes in BOLD fMRI during transition to Stage 1 sleep. When relaxed with eyes-closed, waxing and waning of wakefulness can occur due to a drift into either the drowsy or alert state [6, 29–31]. The transition towards a more alert/attentive state is associated with increased fronto-parietal activity [31]. In contrast, transition to sleep-like states manifests as

increased occipito-parietal activity [31]. By modelling EEG theta-related activity in each individual, we were able to isolate and replicate regionally-specific increased activity during increased EEG theta activity, a pattern of activity typically associated with lower arousal and early sleep in humans [6, 29–31] and other mammals [19].

Application of the RoWDI method, which used the fMRI activity map of EEG theta as a template, detected frequent sleep-like events in the awake and cognitively-active humans exposed to partial sleep loss. Importantly, these events were associated with lowered arousal as confirmed by the analysis of pupillometric and behavioural response data. On average, these sleep-like events, inferred from fMRI alone, were associated with a 20% reduction in pupil size and prolonged reaction times. Sleep-like intrusions are common phenomena during vigilance tasks performed after sleep deprivation [1, 2, 32–34]. Previous studies have used fMRI activity [19, 20, 23] to track the tonic level of alertness in monkeys and humans during resting-state using templates of lowered arousal. In contrast to the previous studies, our approach can detect individual episodes of sleep-like intrusions.

The voxel-wise analysis, using both the sleep-like events detected using RoWDI and task trials in a single model, revealed distinct brain networks active during sleep-like intrusions and task performance. During sleep-like intrusions, increased activity was observed in the somatosensory and limbic areas of the brain, whereas decreased activity was observed in the thalamus and the ventral prefrontal cortices. An fMRI pattern strikingly similar to ours has previously been reported to occur during lowered arousal associated with wake-sleep transitions [19] and during microsleeps [17], further confirming that RoWDI is able to infer sleep-like intrusions in fMRI data. Other neuroimaging studies have corroborated these findings by showing decreased activity in the thalamus during microsleeps [1] and spontaneous slowed eye-closures during drowsiness [18]. The findings are also comparable with previous neuroimaging studies which used pupil diameter as a marker of arousal [11–14, 35]. We found that sleep-like state detected using RoWDI was associated with reduced pupil size. Although such changes in pupil size may also occur due to droopy eyes associated with sleepiness, they are also linked to fluctuations in arousal mediated by changes in brain-stem activity [11–14, 35]. Importantly, some of the fMRI activity during sleep-like events, observed in the somatosensory brain regions, cingulate, and thalamus also matches what has been reported to be correlated with changes pupil size [14, 35]. Such cortico-thalamic activity during a hypoactive behavioural state has been attributed to rich endogenous mental activity that can occur at the wake-sleep transition in humans [17].

Notably, despite the frequent inferred sleep intrusions in the brain, we found that the task-related brain networks were robustly activated. That is, the task-activated brain regions expected to be involved in attention and working memory (frontal and parietal regions), motor (left primary motor), decision-making (Anterior Cingulate Cortex, insula), and alertness/arousal (bilateral thalamus) processes were active despite sleep-like intrusions. Although there was some overlap between sleep-related activation and task-related pattern, particularly in the association cortex, the pattern of deactivation was only observed in sleep-like intrusions. Taken together, these findings suggest that distinct sleep-like brain states can intrude in awake and cognitively active human brain.

Some limitations need to be considered while interpreting our findings. Firstly, our analysis was limited to detecting fMRI activity associated with increased activity in EEG theta. Recent studies have reported that intrusions of local slow-wave sleep can occur in awake humans [36]. The use of slow wave sleep activity as regressors may reveal a different level of sleep intrusions in the awake brain, which will be investigated in future studies. Secondly, our pupil detection algorithm relied on automatic post-processing of eye-video recordings. Thus, when eyes were closed, the pupil size was reported as zero. Therefore, our pupillometric measures likely reflect changes in pupil size associated with drowsiness and sleep onset. We could only measure pupil size when eyes were fully open, which is what was required to perform the task.

In conclusion, this is the first study to describe a method to track sleep-like intrusions in fMRI data via an RoWDI approach. The RoWDI was able to detect sleep-like events in fMRI data acquired during cognitive task performed after partial sleep deprivation, without the need for simultaneous recording of EEG. The RoWDI approach will be useful for removing any artefactual fMRI activations associated with sleep-like intrusions during resting-state or task-related fMRI paradigms.

## Data availability statement

The data that support the findings of this study are available upon reasonable request from the authors.

## Acknowledgments

This research was supported by Faculty of Health Sciences Project Grant, Australian Catholic University, Royal Society of New Zealand Marsden Grant, and Monash University Strategic Grant Scheme.

## ORCID iD

Govinda R Poudel  <https://orcid.org/0000-0002-0043-7531>

## References

- [1] Poudel G R, Innes C R H, Bones P J, Watts R and Jones R D 2014 Losing the struggle to stay awake: divergent thalamic and cortical activity during microsleeps *Hum. Brain Mapp.* **35** 257–69
- [2] Jonmohamadi Y, Poudel G R, Innes C C R H and Jones R D 2016 Microsleeps are associated with stage-2 sleep spindles from hippocampal-temporal network *Int. J. Neural Syst.* **26** 1650015
- [3] Toppi J, Astolfi L, Poudel G R, Innes C R H, Babiloni F and Jones R D 2016 Time-varying effective connectivity of the cortical neuroelectric activity associated with behavioural microsleeps *Neuroimage* **124** 421–32
- [4] Poudel G R, Innes C R H and Jones R D 2018 Temporal evolution of neural activity and connectivity during microsleeps when rested and following sleep restriction *Neuroimage* **174** 263–73
- [5] Weddell S, Ayyagari S and Jones R D 2020 Reservoir computing approaches to microsleep detection *J. Neural Eng.* **18** 046021
- [6] Tagliazucchi E and Laufs H 2014 Decoding wakefulness levels from typical fMRI resting-state data reveals reliable drifts between wakefulness and sleep *Neuron* **82** 695–708
- [7] Sen B and Parhi K K 2021 Predicting biological gender and intelligence from fMRI via dynamic functional connectivity *IEEE Trans. Biomed. Eng.* **68** 815–25
- [8] McAvoy M P, Tagliazucchi E, Laufs H and Raichle M E 2019 Human non-REM sleep and the mean global BOLD signal *J. Cereb. Blood Flow Metab.* **39** 2210–22
- [9] Elliott M L, Knodt A R, Ireland D, Morris M L, Poulton R, Ramrakha S, Sison M L, Moffitt T E, Caspi A and Hariri A R 2020 What is the test-retest reliability of common task-functional MRI measures? New empirical evidence and a meta-analysis *Psychol. Sci.* **31** 792–806
- [10] Ko L W, Komarov O, Lai W-K, Liang W-G and Jung T-P 2020 Eyeblink recognition improves fatigue prediction from single-channel forehead EEG in a realistic sustained attention task *J. Neural Eng.* **17** 036015
- [11] Murphy P R, O'Connell R G, O'Sullivan M, Robertson I H and Balsters J H 2014 Pupil diameter covaries with BOLD activity in human locus coeruleus *Hum. Brain Mapp.* **35** 4140–54
- [12] Yellin D, Berkovich-Ohana A and Malach R 2015 Coupling between pupil fluctuations and resting-state fMRI uncovers a slow build-up of antagonistic responses in the human cortex *Neuroimage* **106** 414–27
- [13] Schneider M, Hathway P, Leuchs L, Sämann P G, Czisch M and Spormaker V I 2016 Spontaneous pupil dilations during the resting state are associated with activation of the salience network *Neuroimage* **139** 189–201
- [14] DiNuzzo M, Mascali D, Moraschi M, Bussu G, Maugeri L, Mangini F, Fratini M and Giove F 2019 Brain networks underlying eye's pupil dynamics *Front. Neurosci.* **13** 965
- [15] Hertig-Godeschalk A et al 2020 Microsleep episodes in the borderland between wakefulness and sleep *Sleep* **43** zsz163
- [16] Boyle L N, Tippin J, Paul A and Rizzo M 2008 Driver performance in the moments surrounding a microsleep *Transp. Res. F* **11** 126–36
- [17] Ong J L, Kong D, Chia T T Y, Tandji J, Thomas Yeo B T and Chee M W L 2015 Co-activated yet disconnected-neural correlates of eye closures when trying to stay awake *Neuroimage* **118** 553–62
- [18] Wang C, Ong J L, Patanaik A, Zhou J and Chee M W L 2016 Spontaneous eyelid closures link vigilance fluctuation with fMRI dynamic connectivity states *Proc. Natl Acad. Sci. USA* **113** 9653–8
- [19] Chang C, Leopold D A, Schölvinck M L, Mandelkow H, Picchioni D, Liu X, Ye F Q, Turchi J N and Duyn J H 2016 Tracking brain arousal fluctuations with fMRI *Proc. Natl Acad. Sci. USA* **113** 4518–23
- [20] Falahpour M, Chang C, Wong C W and Liu T T 2018 Template-based prediction of vigilance fluctuations in resting-state fMRI *Neuroimage* **174** 317–27
- [21] Teng J, Ong J L, Patanaik A, Tandji J, Zhou J H, Chee M W L and Lim J 2019 Vigilance declines following sleep deprivation are associated with two previously identified dynamic connectivity states *Neuroimage* **200** 382–90
- [22] McGlashan E M, Poudel G R, Vidafar P, Drummond S P A and Cain S W 2018 Imaging individual differences in the response of the human suprachiasmatic area to light *Front. Neurol.* **9** 1022
- [23] Goodale S E, Ahmed N, Zhao C, De Zwart J A, Özbay P S, Picchioni D, Duyn J, Englot D J, Morgan V L and Chang C 2021 fMRI-based detection of alertness predicts behavioral response variability *Elife* **10** 62376
- [24] Mullinger K J, Castellone P and Bowtell R 2013 Best current practice for obtaining high quality EEG data during simultaneous fMRI *J. Vis. Exp.* **76** 50283
- [25] Nilsson G, Tamm S, Schwarz J, Almeida R, Fischer H, Kecklund G, Lekander M, Fransson P and Åkerstedt T 2017 Intrinsic brain connectivity after partial sleep deprivation in young and older adults: results from the Stockholm Sleepy Brain study *Sci. Rep.* **7** 9422
- [26] Marzano C, Moroni F, Gorgoni M, Nobili L, Ferrara M and De Gennaro L 2013 How we fall asleep: regional and temporal differences in electroencephalographic synchronization at sleep onset *Sleep Med.* **14** 1112–22
- [27] Li D and Parkhurst D J 2005 Starburst: a robust algorithm for video-based eye tracking *IEEE Computer Society Conf. Computer Vision Pattern Recognition.* **793** 79
- [28] Kaufmann C, Wehrle T C, Holsboer F, Auer D B, Pollmächer T and Czisch M 2006 Brain activation and hypothalamic functional connectivity during human non-rapid eye movement sleep: an EEG/fMRI study *Brain* **129** 655–67
- [29] Laufs H, Walker M C and Lund T E 2007 'Brain activation and hypothalamic functional connectivity during human non-rapid eye movement sleep: an EEG/fMRI study'—its limitations and an alternative approach *Brain* **130** e75 (author reply e76)
- [30] Brodbeck V, Kuhn A, Von Wegner F, Morzelewski A, Tagliazucchi E, Borisov S, Michel C M and Laufs H 2012 EEG microstates of wakefulness and NREM sleep *Neuroimage* **62** 2129–39
- [31] Laufs H, Kleinschmidt A, Beyerle A, Eger E, Salek-Haddadi A, Preibisch C and Krakow K 2003 EEG-correlated fMRI of human alpha activity *Neuroimage* **19** 1463–76
- [32] Poudel G R, Innes C R and Jones R D 2012 Cerebral perfusion differences between drowsy and nondrowsy individuals after acute sleep restriction *Sleep* **35** 1085–96
- [33] Toppi J et al 2012 Time-varying functional connectivity for understanding the neural basis of behavioral microsleeps *Conf. Proc. IEEE Eng. Med. Biol. Soc.* **2012** 4708–11
- [34] Poudel G R, Innes C R and Jones R D 2013 Distinct neural correlates of time-on-task and transient errors during a visuomotor tracking task after sleep restriction *Neuroimage* **77** 105–13
- [35] Mayeli A et al 2020 Integration of simultaneous resting-state electroencephalography, functional magnetic resonance imaging, and eye-tracker methods to determine and verify electroencephalography vigilance measure *Brain Connect.* **10** 535–46
- [36] Andrillon T, Burns A, Mackay T, Windt J and Tsuchiya N 2021 Predicting lapses of attention with sleep-like slow waves *Nat. Commun.* **12** 3657